

Controlled decoherence of a charge qubit in a double quantum dot

Toshimasa Fujisawa^{a)}

NTT Basic Research Laboratories, NTT Corporation, 3-1 Morinosato-Wakamiya, Atsugi 243-0198, Japan and Tokyo Institute of Technology, 2-12-1, O-okayama, Meguro, Tokyo 152-8550, Japan

Toshiaki Hayashi

NTT Basic Research Laboratories, NTT Corporation, 3-1 Morinosato-Wakamiya, Atsugi 243-0198, Japan

Yoshiro Hirayama

NTT Basic Research Laboratories, NTT Corporation, 3-1 Morinosato-Wakamiya, Atsugi 243-0198, Japan and SORST-JST, 4-1-8 Honmachi, Kawaguchi 331-0012, Japan

(Received 18 January 2004; accepted 21 April 2004; published 18 August 2004)

We investigate coherent time evolution of a charge qubit in a semiconductor double quantum dot. A high-speed voltage pulse controls the energy bias and strength of the decoherence of the system. The qubit is effectively isolated from the electrodes in the Coulomb blockade regime, while it is affected by dissipative tunneling processes in the single-electron tunneling regime. We discuss the importance of the controlled decoherence by means of density matrix simulations. © 2004 American Vacuum Society. [DOI: 10.1116/1.1771679]

I. INTRODUCTION

The quantum dynamics of artificial quantum systems has attracted much attention for quantum computing, in which each particle and interactions between particles are sequentially manipulated in a programmable manner.¹ Recent nanofabrication technology allows us to design artificial atoms (quantum dots) and molecules (double quantum dots), in which atomic (molecular)-like electronic states can be controlled with external voltages.²⁻⁵ The eigenstates of interacting electrons in quantum dots can be well understood in terms of atomic physics language, and can be controlled with adjustable parameters. Electron spin and orbital degrees of freedom in quantum dots are interesting for the applications to quantum information devices.^{6,7} Coherent manipulation of the electronic system in quantum dots is crucial for future applications to quantum information technology. In general, longer decoherence time is strongly required in order to perform enough computation steps, while the initial state has to be prepared in a known state that is often chosen to be a ground state. It is desirable to be able to change the strength of the decoherence at will to satisfy the conflicting requirements.

A double quantum dot (DQD) provide a simple and realistic two-level system, which can be discussed with an electron in a double dot potential.⁷ In a classical picture, where the two quantum dots are well isolated, the system can be described by two charge states, in which an electron occupies the left dot or the right dot. When the tunneling between the two dots is allowed, however, the electron wave function can be expressed with a linear superposition of the two localized wave functions. This system is referred to as charge qubit, since this is expected to work as a building block of a quantum computer. It has been shown from various experiments and theoretical studies that the coherent superposition can be prepared and manipulated by adjusting the potential or an

electric field.^{3,8,9} A large electric dipole of a charge qubit can be used to couple with another charge qubit, and two-qubit operation can also be realized with the dipole interaction. In practice, full one-qubit operation has been demonstrated with rotation gate, which changes the probability of finding an electron in one dot, and phase shift gate, which changes the phase difference between the two localized wave functions.¹⁰ In addition to superconducting charge qubits,^{11,12} successful coherent manipulation of the semiconductor charge qubit has indicated the potential applications of a wide variety of semiconductors.

In this article, we focus on the controlled decoherence, in which the strength of decoherence is manipulated in a short time with a pulse. The qubit is effectively isolated from the electrode during the manipulation, while it is influenced by strong decoherence during the initialization and measurement. We discuss the observed oscillation patterns based on simple simulations. Experiments of the coherent manipulation are described in Sec. II, and analysis based on density matrix calculation is shown in Sec. III.

II. CHARGE QUBIT IN A DOUBLE QUANTUM DOT

The DQD used for this work was fabricated in a GaAs/AlGaAs heterostructure with a two-dimensional electron gas. As shown in the scanning electron micrograph in Fig. 1(a), a narrow conductive channel is formed between the etched grooves (the upper and lower dark regions). Three tunneling barriers are formed by applying negative voltages, V_L , V_C , and V_R , to the corresponding metal electrodes (the bright vertical lines), leaving the left and right QDs (white circles) between the source and drain electrodes. The potential of the QDs can also be modified by applying other gate voltages: V_l and V_r . The experiment was performed in a magnetic field of 0.5 T at lattice temperature $T_{\text{lat}} \lesssim 20$ mK.^{8,10} The effective electron temperature, however, remained at $T_{\text{elec}} \sim 100$ mK, probably due to high-frequency noise.

^{a)}Electronic mail: fujisawa@will.brl.ntt.co.jp

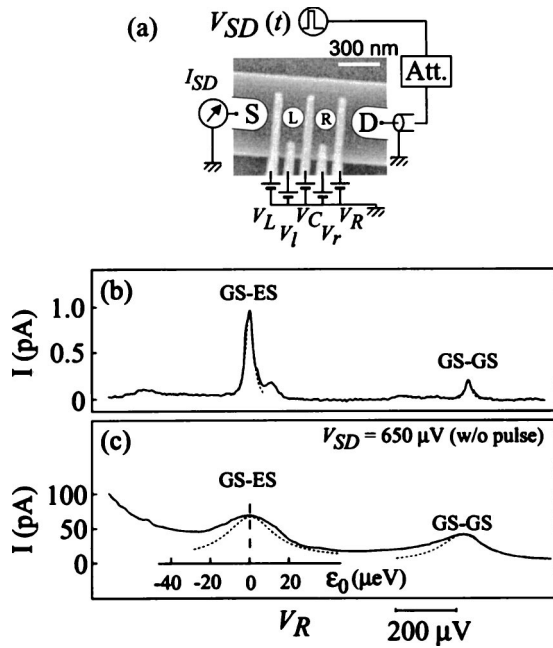


FIG. 1. (a) Schematic of the measurement setup and a scanning electron microscope image of the sample. (b) and (c) Current spectra of a double quantum dot device. Dotted lines are Lorentzian fitting curves.

Each dot shows on-site charging energy of $E_c \sim 1.3$ meV and typical energy spacing of $100 \mu\text{eV}$. The interdot electrostatic coupling energy is $U \sim 200 \mu\text{eV}$. In the weak-coupling regime, finite current is only observed at the triple points, where all tunneling processes through the three tunneling barriers are allowed. Figures 1(b) and 1(c) show the current spectrum near a triple point when V_R is swept. Since a relatively large source–drain voltage, $V_{SD} = 650 \mu\text{V}$ (constant) is applied, a couple of resonant tunneling peaks appear. The right (left) peak is assigned to the resonance of the ground state (the first excited state) of the left dot to the ground state of the right dot. Each peak profile can be fitted with a Lorentzian curve (dotted lines), which is consistent with the density matrix theory [discussed later with Eq. (2)].^{13,14} The horizontal axis can be converted into the energy difference between the two state ϵ_0 , which is indicated for the left resonant peak in Fig. 1(c). From the fitting, the tunneling rate through the left and right barrier Γ_L and Γ_R and tunneling coupling between the two dots T_c are estimated to be $\hbar\Gamma_L \sim \hbar\Gamma_R \sim 0.005 \mu\text{eV}$ and $\hbar T_c \sim 1 \mu\text{eV}$ for Fig. 1(b) and $\hbar\Gamma_L \sim \hbar\Gamma_R \sim 30 \mu\text{eV}$ and $\hbar T_c \sim 1 \mu\text{eV}$ for Fig. 1(c). In the vicinity of each resonant peak, an artificial two-level system (quantum bit) can be defined by considering corresponding two states. An excess electron occupies the left dot ($|L\rangle$) or the right dot ($|R\rangle$). The following experiment is obtained around the left resonant peak in Fig. 1(c).

The qubit state can be initialized, manipulated, and measured by applying a rectangular voltage pulse to the drain electrode. When a large source–drain voltage V_{SD} ($\sim 650 \mu\text{eV}$) is applied, resonant tunneling current is observed as shown in Fig. 1(c). The energy diagram in this situation is schematically shown in Fig. 2(a), where only two

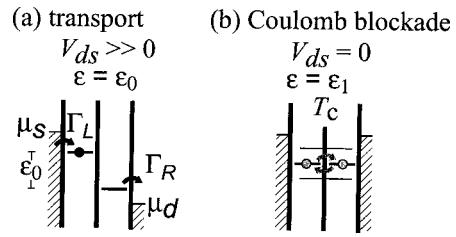


FIG. 2. Schematic energy diagram of the double quantum dot: (a) in the transport regime and (b) in the Coulomb blockade regime.

states are considered for simplicity. Since electrons flow through the DQD, the qubit state is, in general, a statistical mixture of $|L\rangle$, $|R\rangle$, $|0\rangle$ (empty state), and $|2\rangle$ (doubly occupied state). However, the qubit is effectively initialized in the localized state $|L\rangle$ by choosing $\Gamma_L, \Gamma_R \gg T_c$ (discussed later).

When V_{SD} is turned off to zero, the DQD can be adjusted in the Coulomb blockade regime [see Fig. 2(b)]. In this case, the interdot electrostatic coupling prevents electrons from tunneling into and out of the DQD within the first-order tunneling process, and thus no current flows through the DQD. The system prepared in $|L\rangle$ goes back and forth between $|L\rangle$ and $|R\rangle$.

Then, the large bias voltage is restored for the measurement [Fig. 2(a)]. If the oscillation ends up in $|R\rangle$, the electron tunnels out to the drain electrode and contributes to the excess pulse-induced current, while no excess current is expected for $|L\rangle$. This current depends on the probability of $|R\rangle$.

In practice, we repeatedly applied many pulses with a repetition frequency $f_{\text{rep}} = 100$ MHz and measured the average dc current I . The current consists of the coherent pumping current and inelastic current that flows during initialization. In order to improve the signal-to-noise ratio, we employed a lock-in amplifier technique to measure the pulse-induced current I_p by switching the pulse train on and off at a low modulation frequency of 100 Hz. We evaluated the average number of pulse-induced tunneling electrons $\langle n_p \rangle = I_p / ef_{\text{mod}}$.

When the pulse train was applied, the pulse-induced current I_p appeared as shown in Fig. 3(a). The horizontal axis, in which V_R is swept, is converted to the energy difference between the two states ϵ . The upper scale ϵ_0 (lower scale ϵ_1) shows the energy difference when a large $V_{SD} \sim 650 \mu\text{eV}$ (zero voltage) is applied. The origin $\epsilon_0 = 0$ is determined from the peak position in Fig. 1(c), and $\epsilon_1 = 0$ is determined at the maximum amplitude of the oscillation in Fig. 3(a). $\epsilon_1 - \epsilon_0 \sim 30 \mu\text{eV}$ may be reasonable, since the dots are capacitively coupled to the source and drain electrode. The oscillation amplitude and period decreases when the condition is away from the resonance $\epsilon_1 = 0$. The oscillation pattern is not symmetric about $\epsilon_1 = 0$. This can be explained by the nonideal rectangular pulse wave form with a rise time of about 100 ps. The traces at $\epsilon_1 = 0$ and $\epsilon_0 = 0$ are also shown in Figs. 3(b) and 3(c), respectively. It should be noted that

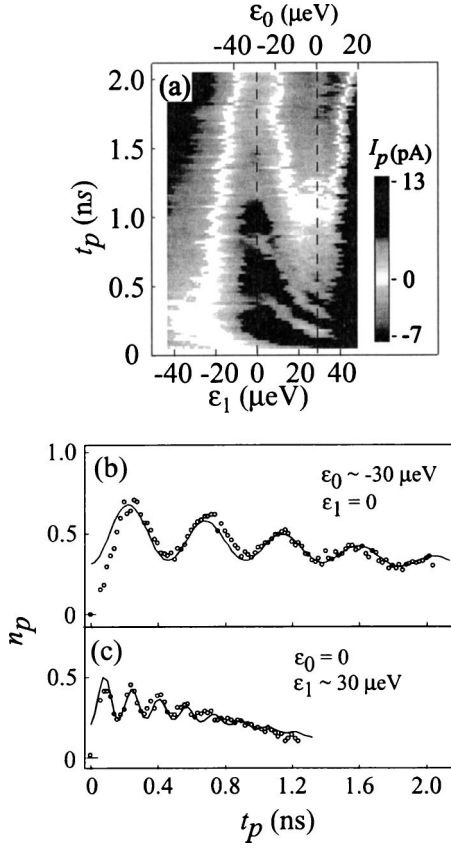


FIG. 3. (a) Plot of the pulse induced current I_p . (b) and (c) Pulse-induced current I_p at $\epsilon_1 \sim 0$ and $\epsilon_0 \sim 0$. The solid lines are damped cosine functions with a linearly decreasing term, which is fitted to the data.

the oscillation is clearly observed even at $\epsilon_0 = 0$, where two levels are resonant during transport but off-resonant during oscillation. In this case, the controlled decoherence plays an important role in the manipulation. We will investigate this effect by means of density matrix simulations.

III. DENSITY MATRIX SIMULATIONS

The transport through a double dot has often been discussed using density matrix calculations.^{13,15} We consider one-electron states in spin-degenerated states $|L\rangle$ and $|R\rangle$ in the DQD. The empty state $|0\rangle$, in which there is no electron in the DQD, and the doubly occupied state $|2\rangle$, in which two electrons occupy different dots, are considered. State $|2\rangle$ has fourfold degeneracy, and the exchange energy (splitting into the spin singlet and triplet) is neglected. Other states, such as two electrons in one dot, are not considered because the onsite Coulomb energy is larger than the energy scale considered here. We consider tunneling transitions between these states, and neglect other decoherence sources for simplicity.

In the nonlinear transport regime, where a relatively large V_{SD} is applied ($U < V_{SD} < E_c$), electrons tunnel through the DQD as shown in Fig. 2(a). The rate equations for the reduced density matrix ρ of the qubit are

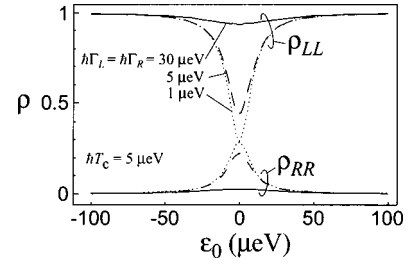


FIG. 4. Density matrix elements ρ_{LL} and ρ_{RR} , calculated for the initial condition.

$$\begin{aligned}
 \dot{\rho}_{LL} &= 2\hbar\Gamma_L\rho_{00} + \hbar\Gamma_R\rho_{22} + i\hbar T_c(\rho_{LR} - \rho_{RL}), \\
 \dot{\rho}_{RR} &= -\hbar(\Gamma_R + \Gamma_L)\rho_{RR} - i\hbar T_c(\rho_{LR} - \rho_{RL}), \\
 \dot{\rho}_{LR} &= -\frac{\hbar}{2}(\Gamma_L + \Gamma_R)\rho_{LR} + i\hbar\epsilon\rho_{LR} + i\hbar T_c(\rho_{LL} - \rho_{RR}), \\
 \dot{\rho}_{RL} &= -\frac{\hbar}{2}(\Gamma_L + \Gamma_R)\rho_{RL} - i\hbar\epsilon\rho_{RL} - i\hbar T_c(\rho_{LL} - \rho_{RR}), \\
 \dot{\rho}_{00} &= -2\hbar\Gamma_L\rho_{00} + \hbar\Gamma_R\rho_{RR}, \\
 \dot{\rho}_{22} &= -\hbar\Gamma_R\rho_{22} + 2\hbar\Gamma_L\rho_{RR},
 \end{aligned} \tag{1}$$

after Gurvitz and Prager.¹⁵ We assumed that Γ_L and Γ_R are independent of the energy and the charge states. The tunnel coupling to the reservoirs gives the decoherence rate, $(\Gamma_L + \Gamma_R)/2$. The steady current I_{st} in the steady state ($\dot{\rho} = 0$) is given by

$$I_{st}/e = \frac{(2\Gamma_L + \Gamma_R)T_c^2}{\epsilon^2 + (2\Gamma_L + \Gamma_R)^2(1/4 + T_c^2/2\Gamma_L\Gamma_R)}, \tag{2}$$

which is useful in roughly estimating T_c , Γ_L , and Γ_R . One can determine these parameters by measuring the height and width of the resonant tunneling current peak in the forward and reverse current directions. We discuss how the initialization and measurement processes work in this regime.

For the initialization, we keep the DQD in the transport regime for enough time [$> 2/(\Gamma_L + \Gamma_R)$] to obtain a steady state ($\dot{\rho} = 0$). Figure 4 shows density matrix elements ρ_{RR} and ρ_{LL} . For $|\epsilon| \gg \hbar T_c$, the steady state is well defined to $|L\rangle$ ($\rho_{LL} \sim 1$) regardless of Γ_L and Γ_R . When Γ_L and Γ_R are greater than T_c (the solid line for the measurement condition of Fig. 2), the localized initial state ($|L\rangle$) is effectively prepared at any ϵ .

The measurement of the qubit works in the transport regime. Suppose the qubit is prepared in a pure state $|\psi\rangle = \cos(\theta/2)|L\rangle + e^{i\phi}\sin(\theta/2)|R\rangle$. The time-dependent tunneling current

$$I_\psi(t) = e\Gamma_R(\rho_{RR} + \rho_{22}) \tag{3}$$

is obtained by solving Eq. (1) under the initial condition $\rho(t=0) = |\psi\rangle\langle\psi|$. The effective total number of tunneling electrons during the measurement process $\langle N \rangle$ is obtained by

$$\langle N \rangle = \frac{1}{e} \int_0^\infty [I_\psi(t) - I_{st}] dt, \tag{4}$$

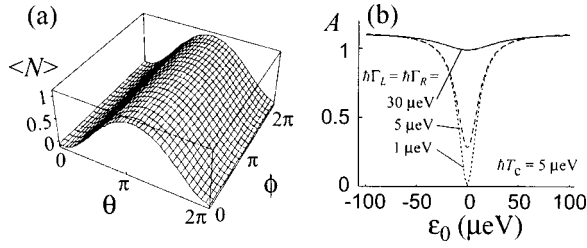


FIG. 5. (a) Expected electron number of the pulse-induced tunneling current and (b) amplitude of the detection signal.

where the static current is subtracted from the total current. Figure 5(a) shows the calculated $\langle N \rangle$ for a specific condition ($\hbar\Gamma_L = \hbar\Gamma_R = \epsilon = 30 \mu\text{eV}$ and $\hbar T_c = 5 \mu\text{eV}$). $\langle N \rangle$ depends only on θ , and its sinusoidal dependence indicates a projection measurement of $|\psi\rangle$. Figure 5(b) shows the amplitude of the signal defined by

$$A = \langle N(\theta = \pi) \rangle - \langle N(\theta = 0) \rangle. \quad (5)$$

The signal amplitude is always high when Γ_L and Γ_R are chosen to be greater than T_c . Thus, the initialization and measurement works when $|\epsilon| \gg \hbar T_c$ or $\Gamma_L, \Gamma_R \gg T_c$.

Next, we consider the DQD in the Coulomb blockade regime, where direct tunneling into and out of the DQD is blocked. Tunneling transition only changes the empty state and the doubly occupied state to the one-electron states. By neglecting higher-order tunneling and other decoherence mechanisms, the rate equations are

$$\begin{aligned} \dot{\rho}_{LL} &= 2\hbar\Gamma_L\rho_{00} + \hbar\Gamma_R\rho_{22} + i\hbar T_c(\rho_{LR} - \rho_{RL}), \\ \dot{\rho}_{RR} &= 2\hbar\Gamma_R\rho_{00} + \hbar\Gamma_L\rho_{22} - i\hbar T_c(\rho_{LR} - \rho_{RL}), \\ \dot{\rho}_{LR} &= i\hbar\epsilon\rho_{LR} + i\hbar T_c(\rho_{LL} - \rho_{RR}), \\ \dot{\rho}_{RL} &= -i\hbar\epsilon\rho_{RL} - i\hbar T_c(\rho_{LL} - \rho_{RR}), \\ \dot{\rho}_{00} &= -2\hbar(\Gamma_L + \Gamma_R)\rho_{00}, \\ \dot{\rho}_{22} &= -\hbar(\Gamma_L + \Gamma_R)\rho_{22}. \end{aligned} \quad (6)$$

In this case, real parts containing Γ_L and Γ_R just build up the qubit state, and coherent time evolution is expected. One can simulate the qubit measurement by solving Eqs. (1) and (6). We calculated the expected value of tunneling electrons $\langle N \rangle$ after the time evolution under various initialization conditions. Figure 6(a) shows the simulation under a realistic condition. The parameters ($\hbar\Gamma_L = \hbar\Gamma_R = 30 \mu\text{eV}$, $\hbar T_c = 5 \mu\text{eV}$, and $\epsilon_1 - \epsilon_0 = 30 \mu\text{eV}$) are adjusted to the experiment in Fig. 3(a), and finite risetime of the pulse is taken into account. The calculation qualitatively coincides with the experiment, implying the validity of the simulation. The experimental data show damping of oscillations, which arises from some decoherence mechanisms not included in the simulation.⁸ However, the asymmetric oscillation pattern is well reproduced in the calculation.

If small tunneling rates ($\hbar\Gamma_L = \hbar\Gamma_R = 1 \mu\text{eV} \ll \hbar T_c$) are assumed, the simulation indicates that the oscillation disappears at $\epsilon_0 \sim 0$ as shown in Fig. 3(b). In this case, bonding and antibonding states, rather than the localized states, are

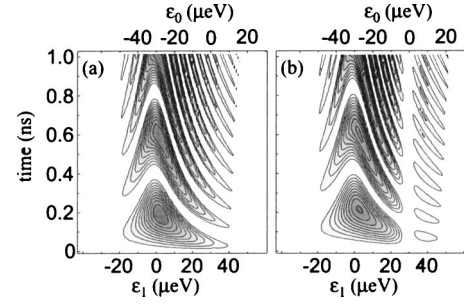


FIG. 6. Intensity plot of the expected electron number when the controlled decoherence is: (a) important and (b) not important. Darkness shows the probability of tunneling electrons (white for zero, black for one).

the eigenstates of the qubit. These eigenstates are equally populated during the initialization (see $\epsilon_0 \sim 0$ in Fig. 4), giving rise to a statistical mixture. Moreover, these eigenstates cannot be effectively measured [see Fig. 5(b)]. Therefore no oscillation is expected in this condition. In contrast, strong dissipative tunneling processes ($\hbar\Gamma_L = \hbar\Gamma_R \gg \hbar T_c$) hold the system in the localized state $|L\rangle$ during the initialization, and provide strong measurement of the localized state $|R\rangle$. Therefore, the clear oscillation that appeared at $\epsilon_0 \sim 0$ is driven by the controlled decoherence in this system.

IV. SUMMARY

We have discussed coherent charge oscillations of a charge qubit in a double quantum dot. The qubit is initialized and measured in the transport regime, where strong decoherence from the tunneling holds the system in the localized state. Then, the qubit is manipulated coherently in the Coulomb blockade regime, where the dissipative tunneling is blocked. The oscillation pattern is well understood by considering this controlled decoherence. This technique may be useful in controlling the qubit state efficiently.

¹M. A. Nielsen and I. L. Chuang, *Quantum Computation and Quantum Information* (Cambridge University Press, Cambridge, 2000).

²S. Tarucha, D. G. Austing, T. Honda, R. J. van der Hage, and L. P. Kouwenhoven, *Phys. Rev. Lett.* **77**, 3613 (1996).

³T. H. Oosterkamp, T. Fujisawa, W. G. van der Wiel, K. Ishibashi, R. V. Hijman, S. Tarucha, and L. P. Kouwenhoven, *Nature* (London) **395**, 873 (1998).

⁴T. Fujisawa, T. H. Oosterkamp, W. G. van der Wiel, B. W. Broer, R. Aguado, S. Tarucha, and L. P. Kouwenhoven, *Science* **282**, 932 (1998).

⁵T. Fujisawa, D. G. Austing, Y. Tokura, Y. Hirayama, and S. Tarucha, *Nature* (London) **419**, 278 (2002).

⁶D. Loss and D. P. DiVincenzo, *Phys. Rev. A* **57**, 120 (1998).

⁷A. Barenco, D. Deutsch, A. Ekert, and R. Jozsa, *Phys. Rev. Lett.* **74**, 4083 (1995).

⁸T. Hayashi, T. Fujisawa, H. D. Cheong, Y. H. Jeong, and Y. Hirayama, *Phys. Rev. Lett.* **91**, 226804 (2003).

⁹A. Balandin and K. L. Wang, *Superlattices Microstruct.* **25**, 509 (1999).

¹⁰T. Fujisawa, T. Hayashi, H. D. Cheong, Y. H. Jeong, and Y. Hirayama, *Physica E* (Amsterdam) **21**, 1046 (2004).

¹¹Y. Nakamura, Yu. A. Pashkin, and J. S. Tsai, *Nature* (London) **398**, 786 (1999).

¹²T. Yamamoto, Yu. A. Pashkin, O. Astafiev, Y. Nakamura, and J. S. Tsai, *Nature* (London) **425**, 941 (2003).

¹³Yu. V. Nazarov, *Physica B* **189**, 57 (1993).

¹⁴N. C. van der Vaart, S. F. Godijn, Yu. V. Nazarov, C. J. P. M. Harmans, and J. E. Mooij, *Phys. Rev. Lett.* **74**, 4702 (1995).

¹⁵S. A. Gurvitz and Ya. S. Prager, *Phys. Rev. B* **53**, 15932 (1996).